





2005

# Dynamics of an inverted pendulum with delayed feedback control

Landry, Maria

SIAM

SIAM J. of Applied Dynamical Systems, V.4, no. 2, Pp. 333-351, 2005.

SIAM J. Applied Dynamical Systems
Vol. 4, No. 2, pp. 333–351


# Dynamics of an Inverted Pendulum with Delayed Feedback Control*

Maria Landry†, Sue Ann Campbell‡, Kirsten Morris§, and Cesar O. Aguilar¶

**Abstract.** We consider an experimental system consisting of a pendulum, which is free to rotate 360 degrees, attached to a cart. The cart can move in one dimension. We describe a model for this system and use it to design a feedback control law that stabilizes the pendulum in the upright position. We then introduce a time delay into the feedback and prove that for values of the delay below a critical delay, the system remains stable. Using a center manifold reduction, we show that the system undergoes a supercritical Hopf bifurcation at the critical delay. Both the critical value of the delay and the stability of the limit cycle are verified experimentally. Our experimental data is illustrated with plots and videos.

**Key words.** inverted pendulum, time delay, feedback control, stability analysis, Hopf bifurcation

**AMS subject classifications.** 70K50, 93D15, 34K18, 34K20, 70Q50

**DOI.** 10.1137/030600461

## 1. Introduction.

In this paper, we examine various aspects of an inverted pendulum system based on the experimental setup depicted schematically in Figure 1. In this system, a pendulum is attached to the side of a cart by means of a pivot which allows the pendulum to swing in the $xy$-plane. A force $F(t)$ is applied to the cart in the $x$ direction, with the purpose of keeping the pendulum balanced upright. See Table 1 for a complete list of notation.

We assume that the pendulum may be modeled as a thin rod. Then, applying Newton's second law to the linear and angular displacement, we arrive at the equations of motion for the system

$$(M+m)\ddot{x} + \epsilon\dot{x} + ml\ddot{\theta}\cos\theta - ml\dot{\theta}^2\sin\theta = F(t), \tag{1.1}$$

$$ml\ddot{x}\cos\theta + \tfrac{4}{3}ml^2\ddot{\theta} - mgl\sin\theta = 0. \tag{1.2}$$

*Received by the editors July 15, 2003; accepted for publication (in revised form) by B. Krauskopf August 13, 2004; published electronically April 14, 2005. S.C. and K.M. acknowledge the support of NSERC through the individual research grants program. M.L. acknowledges the support of NSERC through the USRA program and through the grants of S.C. and K.M. C.A. acknowledges the support of NSERC through the USRA program and of the Department of Applied Mathematics, University of Waterloo.
http://www.siam.org/journals/siads/4-2/60046.html

†Department of Mathematics, University of British Columbia, Room 121, 1984 Mathematics Road, Vancouver, BC V6T 1Z2 Canada (maria@math.ubc.ca).

‡Department of Applied Mathematics, University of Waterloo, Waterloo, ON N2L 3G1, Canada and Centre for Nonlinear Dynamics in Physiology and Medicine, McGill University, Montréal, QC H3A 2T5, Canada (sacampbell@uwaterloo.ca).

§Department of Applied Mathematics, University of Waterloo, Waterloo, ON N2L 3G1, Canada (kmorris@riccati.uwaterloo.ca).

¶Department of Electrical and Computer Engineering, University of Alberta, Edmonton, AB T6G 2V4 Canada (cesar@ece.ualberta.ca).

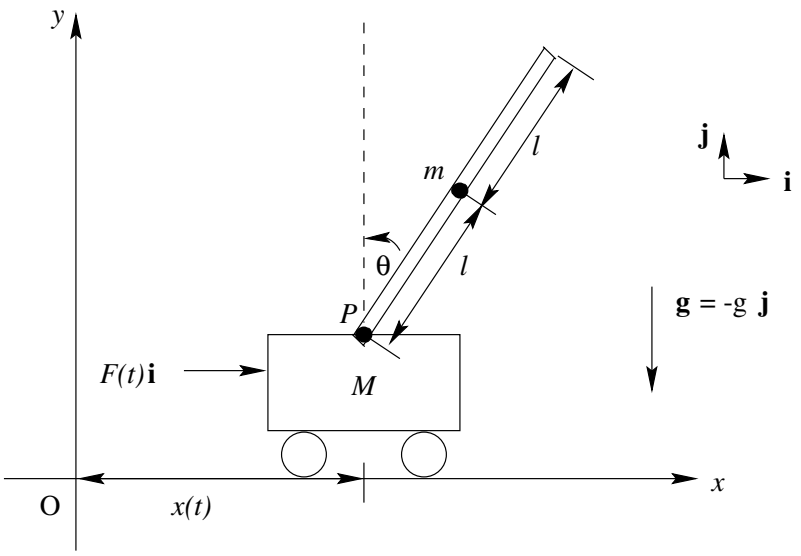


**Figure 1.** *Inverted pendulum system.*

**Table 1**
*Notation.*

| | |
|---|---|
| $x(t)$ | Displacement of the center of mass of the cart from point O |
| $\theta(t)$ | Angle the pendulum makes with the top vertical |
| $M$ | Mass of the cart |
| $m$ | Mass of the pendulum |
| $L$ | Length of the pendulum |
| $l$ | Distance from the pivot to the center of mass of the pendulum ($l = L/2$) |
| $P$ | Pivot point of the pendulum |
| $F(t)$ | Force applied to the cart |

In our experimental setup, the force $F(t)$ on the cart is

$$F(t) = \alpha V(t) - \beta \dot{x}(t), \tag{1.3}$$

where $V(t)$ is the voltage in the motor driving the cart, and the second term represents electrical resistance in the motor. The voltage $V(t)$ can be varied and is used to control the system. The values of the parameters for our experimental setup [21] are given in Table 2. The precise value of the viscous friction $\epsilon$ is difficult to measure; however, we expect that it will be of a similar order of magnitude as $\beta$. Our work will thus consider $\epsilon$ in the range $[0, 15]$.

A more convenient form of the equations is found by solving for $\ddot{x}$ and $\ddot{\theta}$ from equations (1.1) and (1.2) and introducing the variables

$$\begin{aligned} \mathbf{y} &= (y_1, y_2, y_3, y_4)^T \\ &= (x, \theta, \dot{x}, \dot{\theta})^T. \end{aligned} \tag{1.4}$$

**Table 2**
*Values of parameters in experimental system.*

| Parameter | Value | Description |
|---|---|---|
| $w_M$ | 0.360 Kg | Weight mass |
| $M$ | 0.455 Kg + $w_M$ | Mass of the cart |
| $m$ | 0.210 Kg | Mass of the pendulum |
| $L$ | 0.61 m | Length of the pendulum |
| $g$ | 9.8 m/s | Acceleration due to gravity |
| $\epsilon$ | unknown | Viscous friction |
| $K_m$ | 0.00767 V/(rad/sec) | Motor torque and back emf constant |
| $K_g$ | 3.7 | Gearbox ratio |
| $R$ | 2.6 Ω | Motor armature resistance |
| $d$ | 0.00635 m | Motor pinion diameter |
| $\alpha$ | 1.7189 | $(K_m K_g)/(Rd)$ |
| $\beta$ | 7.682 | $\alpha^2 R$ |

We thus obtain the following equivalent first-order system:

$$\dot{\mathbf{y}} = \mathbf{f}(\mathbf{y}) = \begin{pmatrix} y_3 \\ y_4 \\ \dfrac{4F(t) - 4\epsilon y_3 + 4ml y_4^2 \sin y_2 - 3mg \sin y_2 \cos y_2}{4(M+m) - 3m\cos^2 y_2} \\ \dfrac{(M+m)g \sin y_2 - (F(t) - \epsilon y_3)\cos y_2 - ml y_4^2 \sin y_2 \cos y_2}{l(\frac{4}{3}(M+m) - m\cos^2 y_2)} \end{pmatrix}. \tag{1.5}$$

It is well known that for (1.5) with no control ($F(t) = 0$), the cart at rest with the pendulum in the upright position is an unstable equilibrium, while the cart at rest with the pendulum in the downward position is a stable equilibrium. This is reviewed in the next section. In section 3 we apply a feedback control to the system; i.e., the voltage $V(t)$, and hence the force $F(t)$, will be set to a function of the states $x, \theta, \dot{x}, \dot{\theta}$. We show that for the controlled system, the pendulum in the upright position (with the cart at rest) is a stable equilibrium while that in the downward position is now an unstable equilibrium. Finally, we consider the effect of a time delay into the feedback loop. In section 4 we show that for values of delay below a critical value, the equilibrium with the pendulum in the upright position remains stable and above this value this equilibrium becomes unstable. In section 5 we use a center manifold reduction to show that when the upright position loses stability a supercritical Hopf bifurcation takes place, giving rise to a stable limit cycle. These theoretical predictions are confirmed by our experimental results.

The control of the inverted pendulum is a classic problem which has application to both biological and mechanical balancing tasks. As such there have been many papers written on the subject. Here we briefly review the ones most directly related to our work, i.e., those that involve time delayed feedback. Other references can be found within the papers cited. In contrast with our model (1.5) and choice of feedback (section 3), all of these papers eliminate the cart dynamics from the problem by neglecting the viscous friction (and resistance in the cart motor) and using feedback which depends only on $\theta$ and $\dot{\theta}$. Stability analysis of

this second-order equation can be found in the work of Stépán and collaborators [14, 23]. Stépán and Kollár [24] formulate conditions on the delay such that stabilizing controllers can and cannot exist. Atay [1] does a similar analysis employing position feedback only, but with multiple delays. Sieber and Krauskopf [22] show there is a codimension three bifurcation point in the model and use center manifold and normal form analysis to show that this point acts as an organizing center for the dynamics of the system. The emphasis of these studies is on theoretical analysis of the model for arbitrary parameters, whereas we focus on understanding the model with the parameters dictated by our experimental setup. Finally, we note the work of Cabrera and Milton [2, 3], who study, theoretically and experimentally, an inverted pendulum where the control is provided by a person (the "stick balancing problem"). The emphasis of this work is on the interplay between the time delay and the noise in the system.

## 2. Stability of the uncontrolled system.

Consider the inverted pendulum system as given by (1.5). When there is no control applied, i.e., $F(t) = 0$, every point $\bar{\mathbf{y}}$ of the form

$$\bar{\mathbf{y}} = (c, n\pi, 0, 0)^T, \qquad c \in \mathbb{R}, \quad n = 0, \pm 1, \pm 2, \ldots,$$

is an equilibrium point of the system. The equilibria with $n$ even correspond to the upright position of the pendulum and those with $n$ odd to the downward position. Note that the equilibria are not isolated but lie on lines parallel to the $y_1$-axis. This is a consequence of the equivariance of $\mathbf{f}(\mathbf{y})$ with respect to the Euclidean group acting on the first coordinate of $\mathbf{y}$. (In physical terms, our model (1.1)–(1.2) is unchanged by arbitrary reflections and translations in the variable $x$.) The lines correspond to group orbits of equilibria.

In this and the following sections, we will make use of the linearization of (1.5) about the equilibrium $\mathbf{y} = \bar{\mathbf{y}}$,

$$\dot{\mathbf{u}} = D\mathbf{f}(\bar{\mathbf{y}})\mathbf{u}, \tag{2.1}$$

where $\mathbf{u} = \mathbf{y} - \bar{\mathbf{y}}$. Recall that the linear stability of an equilibrium point $\bar{\mathbf{y}}$ is determined by the eigenvalues of the Jacobian matrix $D\mathbf{f}(\bar{\mathbf{y}})$. To study these eigenvalues we will use the Routh–Hurwitz criterion, e.g., [17, pp. 82–85]. Stated for the specific case of a cubic polynomial, it is as follows.

Proposition 1. *Consider the cubic polynomial*

$$a_0\lambda^3 + a_1\lambda^2 + a_2\lambda + a_3,$$

*where $a_i$ are all real. A necessary condition for all the roots of the polynomial to be in the left-half-plane is that all the $a_i$ be nonzero and have the same sign. Define $b_1 = a_2 - a_0a_3/a_1$. The number of roots of the polynomial with positive real parts is equal to the number of sign changes in the sequence $a_0, a_1, b_1, a_3$.*

### 2.1. Downward position: $n$ odd.

For $n$ odd, it follows from (1.5) that

$$D\mathbf{f}(\bar{\mathbf{y}}) = \begin{pmatrix} 0 & 0 & 1 & 0 \\ 0 & 0 & 0 & 1 \\ 0 & -3\dfrac{mg}{m+4M} & -4\dfrac{\epsilon}{m+4M} & 0 \\ 0 & -3\dfrac{(M+m)g}{l(m+4M)} & -3\dfrac{\epsilon}{l(m+4M)} & 0 \end{pmatrix}.$$

It is easy to see that $D\mathbf{f}(\bar{\mathbf{y}})$ has a zero eigenvalue corresponding to the direction along the line of equilibria. Thus the equilibria on this line will not be asymptotically stable. However, applying [9, Theorem 4.3] they will be *orbitally asymptotically stable* if the rest of the eigenvalues of $D\mathbf{f}(\bar{\mathbf{y}})$ have negative real parts.

The nonzero eigenvalues are the roots of the cubic

$$\lambda^3 + \frac{4\epsilon}{m+4M}\lambda^2 + \frac{3(M+m)g}{l(m+4M)}\lambda + \frac{3g\epsilon}{l(m+4M)} = 0.$$

For all positive values of the parameters, $a_j > 0$, $j = 0, \ldots, 3$, and $b_1 = \frac{9mg}{4l(m+4M)} > 0$. Thus, by Proposition 1, all the roots of the polynomial have negative real parts. We conclude that the $\bar{\mathbf{y}}$ are orbitally asymptotically stable when $n$ is odd. This means [9] that if $\mathbf{y}(0)$ is sufficiently close to $\bar{\mathbf{y}}$ for some odd $n$, then $y(t)$ approaches some point on the line $(c, n\pi, 0, 0)$ as $t \to \infty$.

**2.2. Upright position: $n$ even.** For $n$ even,

$$D\mathbf{f}(\bar{\mathbf{y}}) = \begin{pmatrix} 0 & 0 & 1 & 0 \\ 0 & 0 & 0 & 1 \\ 0 & -3\dfrac{mg}{m+4M} & -4\dfrac{\epsilon}{m+4M} & 0 \\ 0 & 3\dfrac{(M+m)g}{l(m+4M)} & 3\dfrac{\epsilon}{l(m+4M)} & 0 \end{pmatrix}. \tag{2.2}$$

The characteristic equation for $D\mathbf{f}(\bar{\mathbf{y}})$ is

$$\lambda\left(\lambda^3 + \frac{4\epsilon}{m+4M}\lambda^2 - \frac{3(M+m)g}{l(m+4M)}\lambda - \frac{3g\epsilon}{l(m+4M)}\right) = 0. \tag{2.3}$$

So, as for the equilibria corresponding to the downward position, there is always one zero root. Consider the cubic polynomial which is the second factor of (2.3). For all positive values of the parameters, $a_0, a_1 > 0$, $a_2, a_3 < 0$, and $b_1 = -\frac{9mg}{4l(m+4M)} < 0$. Thus, by Proposition 1, the polynomial has one root with positive real part. We conclude, as expected, that the equilibria $\bar{\mathbf{y}}$ with $n$ even are unstable.

**3. Stability of the controlled system.** Consider the inverted pendulum system as given by (1.5). As shown in the last section, the upright pendulum state $\mathbf{y} = \mathbf{0}$ is an unstable equilibrium point when there is no control applied. In this section we will use the linearized model to design a controller so that this point becomes a locally stable equilibrium point.

Using (2.2), the linearization of system (1.5) about $\mathbf{y} = \mathbf{0}$ is given by

$$\dot{\mathbf{y}}(t) = \begin{pmatrix} 0 & 0 & 1 & 0 \\ 0 & 0 & 0 & 1 \\ 0 & -3\dfrac{mg}{m+4M} & -4\dfrac{\epsilon}{m+4M} & 0 \\ 0 & 3\dfrac{(M+m)g}{l(m+4M)} & 3\dfrac{\epsilon}{l(m+4M)} & 0 \end{pmatrix} \mathbf{y}(t) + \begin{pmatrix} 0 \\ 0 \\ \dfrac{4}{(m+4M)} \\ -\dfrac{3}{l(m+4M)} \end{pmatrix} F(t). \tag{3.1}$$

As described in the introduction, the force $F(t)$ on the cart is

$$F(t) = \alpha V(t) - \beta \dot{x}(t) = \alpha V(t) - \beta y_3(t), \tag{3.2}$$

where $V(t)$ is the voltage in the motor driving the cart, and the second term represents electrical resistance in the motor.

Define the control vector $\mathbf{b} = (0, 0, \frac{4\alpha}{(m+4M)}, -\frac{3\alpha}{l(m+4M)})^T$ and the system matrix

$$A = \begin{pmatrix} 0 & 0 & 1 & 0 \\ 0 & 0 & 0 & 1 \\ 0 & -3\dfrac{mg}{m+4M} & -4\dfrac{(\beta+\epsilon)}{m+4M} & 0 \\ 0 & 3\dfrac{(M+m)g}{l(m+4M)} & 3\dfrac{\beta+\epsilon}{l(m+4M)} & 0 \end{pmatrix}. \tag{3.3}$$

The model for the controlled system linearized about the upright position can be written

$$\dot{\mathbf{y}} = A\mathbf{y} + \mathbf{b}V(t). \tag{3.4}$$

We solved a linear quadratic control problem in order to design the control $V(t)$ so that the upright position becomes a stable equilibrium point as described in, e.g., [17]. Consider the linear quadratic cost functional

$$\inf_{V(t)\in L_2(0,\infty)} \int_0^\infty \left[\mathbf{y}(t)^T Q \mathbf{y}(t) + rV(t)^2\right] dt.$$

The weights $Q \geq 0$ and $r > 0$ are chosen to reflect the relative importance of reducing the states $\mathbf{y}$ and the cost of the control $V$. The solution to this problem is the feedback law

$$V(t) = -r^{-1}\mathbf{b}^T P \mathbf{y}(t),$$

where $P$ is the unique symmetric positive-definite solution to the algebraic Riccati equation

$$A^T P + PA - P\mathbf{b}r^{-1}\mathbf{b}^T P + Q = 0.$$

This feedback is guaranteed to lead to a controlled system where the upright position is a locally stable equilibrium point.

The Riccati equation may be solved numerically for given values for $A$, $\mathbf{b}$, $r$, and $Q$. We used the physical parameter values of Table 2. Experimental work indicated that $\epsilon = 2.1$ is a reasonable estimate for the viscous friction. Using the best model available is important in controller design since modeling errors degrade the system performance, sometimes to the extent of instability. It is not always sufficient to use an underestimate of damping, since *increasing* damping from a nominal value may sometimes lead to instability; see, e.g., [18]. The analysis below verifies that the control law chosen stabilizes the system for a range of values of $\epsilon$ which includes the physically reasonable values.

Since the system is linear and single-input, the control weight $r$ can be absorbed into the state weight $Q$ and was set to 1. The state weight $Q$ was chosen to penalize the positions heavily with small costs on the velocities. This choice of weights penalizes nonzero

position so that the resulting controller will maintain the pendulum near the upright position. Reducing the velocities to zero is a secondary objective. The particular choice of diagonal $Q = \mathrm{diag}(5000, 3000, 20, 20)$ within these considerations is somewhat arbitrary. These choices lead to the feedback law

$$V(t) = \mathbf{k} \cdot \mathbf{y} \tag{3.5}$$

with the feedback gain

$$\mathbf{k} = (70.7107, 142.5409, 50.6911, 26.9817). \tag{3.6}$$

To find the other equilibrium points of the controlled system, put $F(t) = \alpha V(t) - \beta y_3(t)$ with $V(t) = \mathbf{k} \cdot \mathbf{y}$ in (1.5). It is then easy to show that the equilibrium points are given by

$$\bar{\mathbf{y}}_n = \left( -\frac{k_2}{k_1} n\pi, n\pi, 0, 0 \right)^T, \qquad n = 0, \pm 1, \pm 2, \ldots. \tag{3.7}$$

The equilibrium points $\bar{\mathbf{y}}_n$ with $n$ even correspond to the pendulum in the upright position, while those with odd values of $n$ correspond to the pendulum in the downward position.

As mentioned above, the feedback law (3.6) is guaranteed to lead to a controlled system that is locally stable about the upright position, with a damping parameter $\epsilon = 2.1$. We will show that the controlled system is locally stable in this position over a range of values for the damping parameter $\epsilon$. Let $d_i$, $i = 1, \ldots, 4$, indicate the components of the vector $\mathbf{d} = \alpha \mathbf{k}$. Then, using (3.2) and (3.5), the force $F(t)$ can be written

$$F(t) = \mathbf{d} \cdot \mathbf{y} - \beta y_3. \tag{3.8}$$

Consider the linearization of the system (1.5) about any upright equilibrium point $\bar{\mathbf{y}}_{2k}$, $k \in \mathbb{Z}$, with $F(t)$ given by the feedback law (3.8). We obtain

$$D\mathbf{f}(\bar{\mathbf{y}}_{2k}) = \begin{pmatrix} 0 & 0 & 1 & 0 \\ 0 & 0 & 0 & 1 \\ 4\dfrac{d_1}{m+4M} & \dfrac{4d_2 - 3mg}{m+4M} & 4\dfrac{d_3 - (\beta+\epsilon)}{m+4M} & 4\dfrac{d_4}{m+4M} \\ -3\dfrac{d_1}{l(m+4M)} & 3\dfrac{(M+m)g - d_2}{l(m+4M)} & 3\dfrac{\beta+\epsilon-d_3}{l(m+4M)} & -3\dfrac{d_4}{l(m+4M)} \end{pmatrix}.$$

We will show that $\bar{\mathbf{y}}_{2k}$ is a locally asymptotically stable equilibrium point by showing that all the eigenvalues of $D\mathbf{f}$ above have negative real parts. Since the parameter $\epsilon$ is unknown, the eigenvalues of $D\mathbf{f}(\bar{\mathbf{y}}_{2k})$ are functions of $\epsilon$. Figure 2 shows $\mathrm{Re}(\lambda_i)(\epsilon)$, $i = 1, \ldots, 4$, using the parameter values in Table 2. Note that $\mathrm{Re}(\lambda_3)(\epsilon) = \mathrm{Re}(\lambda_4)(\epsilon)$. Also $\mathrm{Re}(\lambda_1)(\epsilon) = \mathrm{Re}(\lambda_2)(\epsilon)$ until about $\epsilon = 2$, where they branch off. The Routh–Hurwitz criterion can be used to verify that for the given parameter values,

$$\mathrm{Re}\,(\lambda_i(\epsilon)) < 0, \ i = 1, \ldots, 4, \quad \text{for} \quad 0 \le \epsilon < 55.2.$$

Therefore, the upright equilibrium points $\bar{\mathbf{y}}_{2k}$ are locally asymptotically stable equilibrium points if $0 \le \epsilon < 55.2$. This certainly includes all physically reasonable values of $\epsilon$; thus we

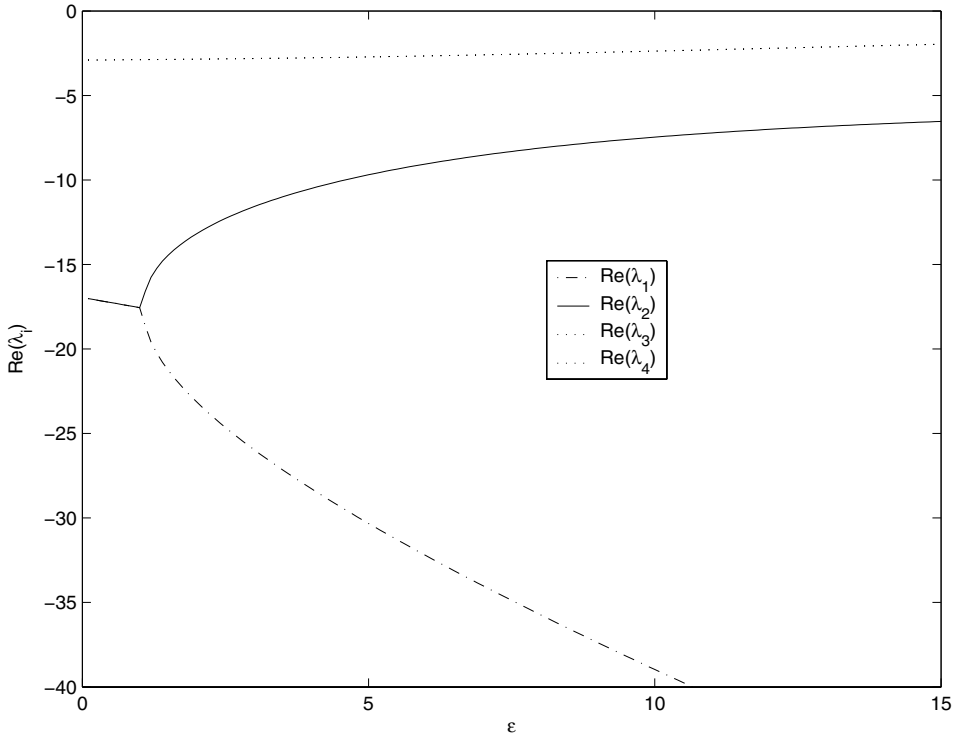


**Figure 2.** *Real parts of the four eigenvalues for the equilibria with the pendulum in the upright position, control applied.*

can be confident that $\bar{\mathbf{y}}_{2k}$ will be locally asymptotically stable in the experimental setting. As was the object of the controller design, applying the feedback control $F(t)$ changes the upright position $\theta = n\pi$, $n$ even, from a locally unstable equilibrium to a locally asymptotically stable equilibrium.

Experimental results are shown in Figure 3. Even at steady-state there is a small-amplitude persistent oscillation. This oscillation is periodic with frequency 2.2 rad/s. Since the sampling time is very small compared to the system dynamics (50 ms) and the oscillations are periodic, this does not appear to be a chaotic response to quantized digital control as observed in [6] and studied in [12]. A possible cause of the oscillations is the presence of a pair of closed-loop eigenvalues in the linearized system with small real and imaginary parts $\lambda \approx -2.3 \pm 2.5i$. If this mode is excited, it would lead to oscillations close to the observed frequency. A possible source of excitation of this mode is noise in the experimental apparatus. There is a filter that attenuates the effects of high frequency noise; however, low frequency components are not attenuated. Another possible cause for these oscillations is the presence of "stiction" or other unmodeled friction in the experimental apparatus. This unmodeled nonlinear effect would lead to overshoot by the linear feedback. Such behavior was predicted theoretically in a balancing system with backlash [14]. It was also observed experimentally in a similar balancing apparatus by Hirschorn and Miller [13]. Friction-generated limit cycles are also shown in simulations of a simple cart system [20].

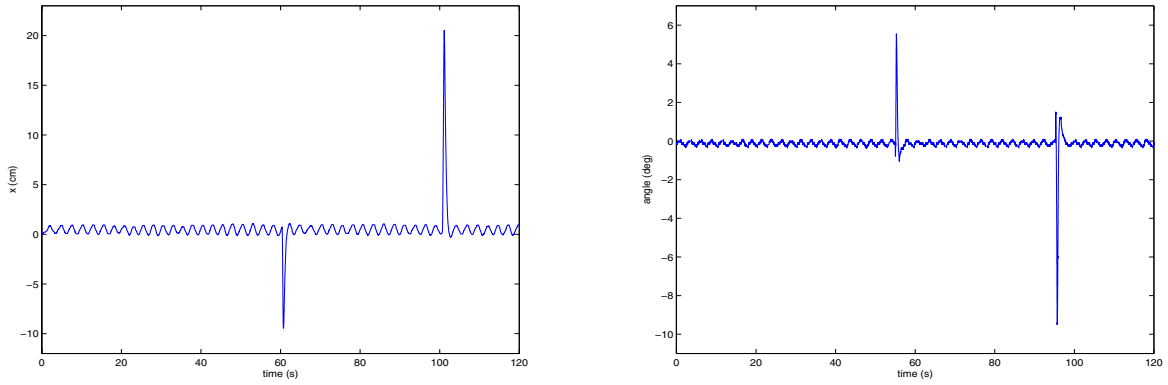


(a) Position (b) Angle

**Figure 3.** *Data for the experimental system with no time delay. Initial conditions close to an equilibrium with the pendulum upright were chosen. The system was perturbed, by giving a small tap to the pendulum, at* $t \approx 60s$ *and* $t \approx 100s$. *Clicking on the above image displays the associated movie* (60046_01.mpg).

In a similar manner, it may be shown that the matrix $D\mathbf{f}(\bar{\mathbf{y}}_{2k+1})$ has an eigenvalue with positive real part, for the parameter values in Table 2 and $0 \leq \epsilon \leq 100$, which includes all physically reasonable values of the damping parameter. Thus, the equilibrium points corresponding to the pendulum in the downward position are unstable. Applying the control $F(t)$ changes the downward position from a locally stable equilibrium into a locally unstable equilibrium.

**4. Effect of time delay.** Consider the system given by (1.1) and (1.2) with $\theta$ close to 0. We have seen in section 3 that the equilibrium point at $\theta = 0$ is locally asymptotically stable when the feedback controlled voltage (3.5) is applied. In this section we will study the effect of time delay in the feedback law.

We assume that there is a time delay $\tau$ between when the variables used in the feedback law (3.5) are measured and when the voltage $V(t)$ is applied. This leads to the new expression

$$V(t) = \mathbf{k} \cdot \mathbf{y}(t - \tau). \tag{4.1}$$

In the experimental system, the actual time delay $\tau$ is insignificant; however, we can artificially increase the delay in the feedback loop.

Using (4.1), (3.8), (1.4), and (1.5) shows that the system is now modeled by the nonlinear delay differential equation

$$\dot{\mathbf{y}}(t) = \mathbf{f}(\mathbf{y}(t), \mathbf{y}(t - \tau)), \tag{4.2}$$

where

$$\mathbf{f}(\mathbf{y}(t),\mathbf{y}(t-\tau)) = \begin{pmatrix} 0 \\ 0 \\ 4 \\ \dfrac{}{4(M+m)-3m\cos^2 y_2(t)} \\ -\dfrac{3\cos y_2(t)}{l(4(M+m)-3m\cos^2 y_2(t))} \end{pmatrix} \sum_{j=1}^{4} d_j y_j(t-\tau) + \begin{pmatrix} y_3(t) \\ y_4(t) \\ \dfrac{-4(\beta+\epsilon)y_3(t)+4ml y_4(t)^2\sin y_2(t)-3mg\sin y_2(t)\cos y_2(t)}{4(M+m)-3m\cos^2 y_2(t)} \\ \dfrac{(M+m)g\sin y_2(t)+(\beta+\epsilon)y_3(t)\cos y_2(t)-ml y_4(t)^2\sin y_2(t)\cos y_2(t)}{l(\frac{4}{3}(M+m)-m\cos^2 y_2(t))} \end{pmatrix}. \tag{4.3}$$

It is easy to check that this equation has the same equilibria as (1.5) and that its linearization about $\mathbf{y}=\mathbf{0}$ is

$$\dot{\mathbf{y}}(t) = A\mathbf{y}(t) + B\mathbf{y}(t-\tau), \tag{4.4}$$

where $A$ is given by (3.3) and

$$B = \begin{pmatrix} 0 & 0 & 0 & 0 \\ 0 & 0 & 0 & 0 \\ \dfrac{4d_1}{m+4M} & \dfrac{4d_2}{m+4M} & \dfrac{4d_3}{m+4M} & \dfrac{4d_4}{m+4M} \\ -\dfrac{3d_1}{(m+4M)l} & -\dfrac{3d_2}{(m+4M)l} & -\dfrac{3d_3}{(m+4M)l} & -\dfrac{3d_4}{(m+4M)l} \end{pmatrix}. \tag{4.5}$$

One might expect that if the time delay is sufficiently large, the feedback will not be able to "keep up" with the system, and the equilibrium at $\theta=0$ will become unstable. We will show that this is true, both theoretically and experimentally. We first calculate the theoretical value of the critical destabilizing delay. We then corroborate this value of the critical delay by introducing delay in the feedback loop in our experimental apparatus.

To study the stability of (4.4) we look for solutions of the form $\mathbf{y}(t)=\mathbf{v}e^{\lambda t}$. Substituting this into (4.4) and then dividing by $e^{\lambda t}$ yield

$$\lambda\mathbf{v} = A\mathbf{v} + B\mathbf{v}e^{-\lambda\tau}.$$

Nontrivial solutions $\mathbf{v}\neq\mathbf{0}$ will exist when $\det(A+Be^{-\lambda\tau}-\lambda I)=0$. Defining

$$P(\lambda;\epsilon) = \frac{l}{3}(m+4M)\lambda^4 + \frac{4l}{3}(\beta+\epsilon)\lambda^3 - (M+m)g\lambda^2 - (\beta+\epsilon)g\lambda,$$
$$Q(\lambda) = \left(d_4 - \frac{4l}{3}d_3\right)\lambda^3 + \left(d_2 - \frac{4l}{3}d_1\right)\lambda^2 + d_3 g\lambda + d_1 g,$$

this condition can be written as

$$P(\lambda;\epsilon) + e^{-\lambda\tau}Q(\lambda) = 0. \tag{4.6}$$

Equation (4.6) is the characteristic equation for the delay differential equation (4.4).

We now make use of some standard results from the stability theory of delay differential equations [5, 15]. It was shown in section 3 that when $\tau = 0$ all roots of (4.6) have negative real parts. Thus, for $\tau > 0$ sufficiently small, all roots of (4.6) have negative real parts. The critical delay is the smallest positive value of $\tau$ where (4.6) has a root with zero real part. At this value of $\tau$ the trivial solution will lose stability.

Defining

$$G(\lambda;\epsilon) = -\frac{Q(\lambda)}{P(\lambda;\epsilon)},$$

(4.6) can be rewritten as

$$G(\lambda;\epsilon) = e^{\lambda\tau}. \tag{4.7}$$

Pure imaginary roots of (4.6) exist when (4.7) is satisfied for $\lambda = i\omega$, $\omega \in \mathbb{R}$. Thus, for a given value of damping $\epsilon$, we need to find the value(s) of $\omega$ such that

$$|G(i\omega;\epsilon)| = 1. \tag{4.8}$$

The corresponding values of $\tau$ are obtained from

$$\tau = \frac{1}{\omega}\left[\arg\{G(i\omega;\epsilon)\} + 2k\pi\right]. \tag{4.9}$$

The critical delay, $\tau_c$, is the smallest positive value of $\tau$ satisfying (4.9). The critical frequency $\omega_c$ is the corresponding value of $\omega$. For the undamped case ($\epsilon = 0$) we found that $\omega_c \approx 31.178$ and $\tau_c \approx 0.0413$. For $0 \le \epsilon \le 15$, the critical value of the delay ranged from .0413 to .075, as shown in Figure 4. We see that friction has a small effect on the critical delay.

Experimental tests were run to determine the experimental critical delay, and it was found to be $\tau_c \approx 0.062$. This value corresponds to $\epsilon \approx 10.6$. With these parameter values the characteristic equation (2.3) has a pair of pure imaginary roots as well as a pair at approximately $-2.7 \pm 2.37i$.

Figures 3, 5, and 6 illustrate the behavior of the system at delays below and above the critical value. In all these cases the initial conditions were chosen so that the system was near the upright equilibrium. The pendulum was perturbed by a small tap in order to illustrate the stability or instability of the equilibrium point. For values below the critical delay (Figures 3 and 5) the system returns to the zero equilibrium after perturbation, illustrating the stability of this equilibrium point. There are small oscillations around zero in all the experiments. These are likely due to the same causes as the persistent oscillations in the undelayed system discussed in section 3: low frequency noise that is exciting the stable mode corresponding to the roots of the characteristic equation with small negative real part and nonzero imaginary part and/or the presence of stick-slip friction between the cart and the track.

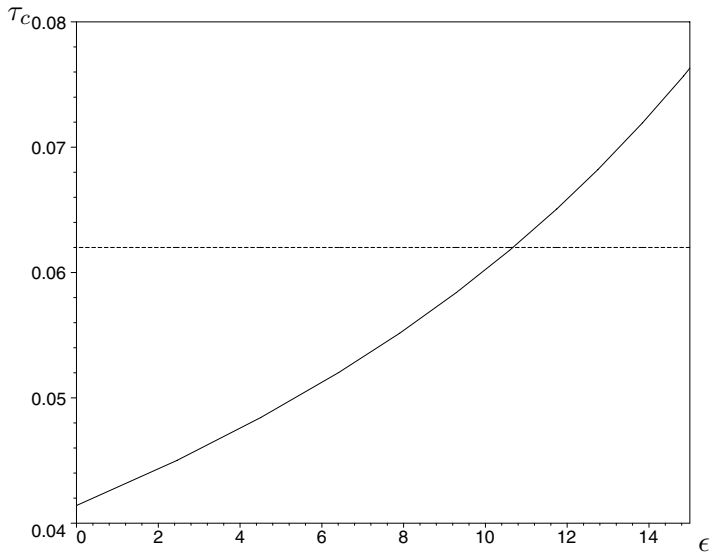


**Figure 4.** *Critical time delay, $\tau_c$, as a function of the damping parameter, $\epsilon$. The experimentally observed value is indicated by the dashed line.*

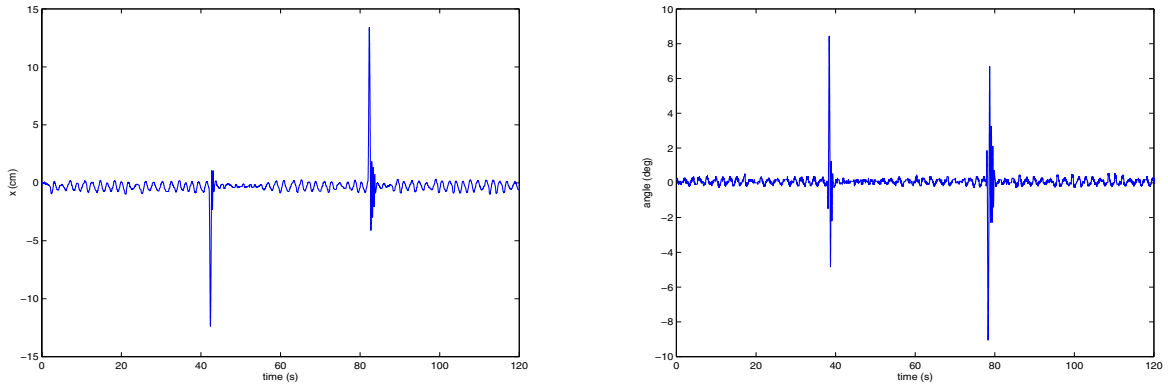


(a) Position (b) Angle

**Figure 5.** *Data for the experimental system with .060s time delay. Initial conditions close to an equilibrium with the pendulum upright were chosen. The system was perturbed, by giving a small tap to the pendulum, at $t \approx 40s$ and $t \approx 80s$. Clicking on the above image displays the associated movie* (60046_02.mpg).

Consider now a delay above the critical delay (Figure 6). After a perturbation, there is a transient, and the system then approaches a limit cycle. After another perturbation, the system returns to the limit cycle. This indicates the presence of a stable limit cycle. This suggests that there is a supercritical Hopf bifurcation at the critical value of the delay. This observation is verified theoretically in the next section using center manifold analysis.

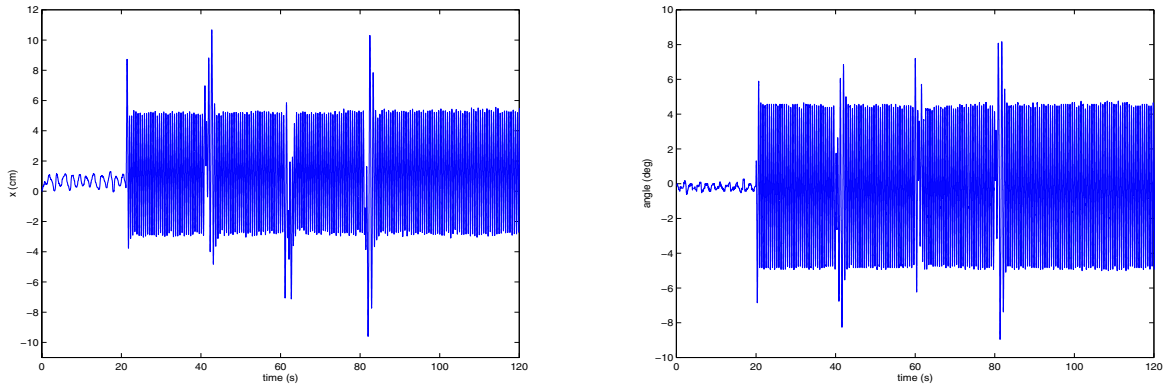


(a) Position (b) Angle

**Figure 6.** *Data for the experimental system with .064s time delay. Initial conditions close to an equilibrium with the pendulum upright were chosen. The system was perturbed, by giving a small tap to the pendulum, at $t \approx 20s$, $t \approx 40s$, $t \approx 60s$, and $t \approx 80s$. Clicking on the above image displays the associated movie* (60046_03.mpg).

**5. Hopf bifurcation.** The previous section showed that the trivial solution of (4.2), i.e., the upright equilibrium, loses stability when $\tau = \tau_c$, as given in (4.9). At such points, the characteristic equation of the linearization (4.4) has a pair of pure imaginary eigenvalues $\pm i\omega_c$, as defined by (4.8). It is straightforward to check that the delay differential equation (4.2) satisfies the conditions for a Hopf bifurcation to occur at each of these points. See [11, pp. 331–333] for a statement of a Hopf bifurcation theorem for delay differential equations. In this section we will determine whether this bifurcation is supercritical, i.e., gives rise to a stable limit cycle as the equilibrium becomes unstable, or subcritical, i.e., loses an unstable limit cycle as the equilibrium becomes unstable.

To study the criticality of the Hopf bifurcation, it is useful to view the solutions of (4.2) and (4.4) as evolving in $C([-\tau, 0], \mathbb{R}^4)$, the space of continuous functions mapping the interval $[-\tau, 0]$ into $\mathbb{R}^4$. Despite the infinite-dimensionality of this space, many of the properties of solutions of delay differential equations such as (4.2) are similar to those for ordinary differential equations. In particular, as described in [11] we have the following. At a Hopf bifurcation point, there exists a two-dimensional center manifold in the solution space. Further, if all the other roots of the characteristic equation of the linearization about the equilibrium have negative real parts, then this manifold is attracting and the long term behavior of solutions to the nonlinear delay differential equation is well approximated by the flow on this manifold. As discussed in [8, 28], the criticality of the Hopf bifurcation can be determined by studying the dynamics on the center manifold. We note that since the manifold is finite-dimensional, the dynamics on it will be described by a system of ordinary differential equations. In this section we will find this system of ordinary differential equations.

Expanding $\mathbf{f}$ in (4.2) in a Taylor series about $\mathbf{y} = 0$, we can rewrite the system in the form

$$\dot{\mathbf{y}} = A\mathbf{y}(t) + B\mathbf{y}(t-\tau) + \mathbf{F}\left(\mathbf{y}(t), \mathbf{y}(t-\tau)\right), \tag{5.1}$$

where $\mathbf{F}$ contains the nonlinear terms and is $O(\mathbf{y}^3)$. It has been shown in [19, 28] that when the lowest order terms in the nonlinearity of the delay equation are of third order (i.e., of the same order as the lowest order terms in the normal form of the Hopf bifurcation), the dynamical system of the center manifold is determined to third order by projecting the delay differential equation onto the subspace, $P$, of solutions of (4.4) corresponding to the eigenvalues $\lambda = \pm i\omega_c$. In fact, it can be shown that the dynamical system, accurate to $O(\mathbf{W}^3)$, is [19, 28]

$$\dot{\mathbf{W}}(t) = \mathbf{M}\mathbf{W}(t) + \Psi(0)\mathbf{F}\left(\Phi(0)\mathbf{W}(t), \Phi(-\tau_c)\mathbf{W}(t)\right), \tag{5.2}$$

where $\mathbf{F}$ is as in (5.1), $\mathbf{M} = \left(\begin{smallmatrix} i\omega_c & 0 \\ 0 & -i\omega_c \end{smallmatrix}\right)$, $\Phi(s)$ is a basis for $P$, $\mathbf{W}(t) = (z(t), \bar{z}(t))^T$, and $z(t)$ is a complex variable. $\Psi(s)$ is a basis for the linear subspace, corresponding to $P$, of the (formal) adjoint problem of (4.4) defined with respect to the scalar product

$$\langle \psi(s), \phi(s) \rangle = \psi(0) \cdot \phi(0) + \int_{-\tau_c}^{0} \psi(s + \tau_c) B \phi(s)\, ds. \tag{5.3}$$

We thus need to do the following: (1) calculate $\Phi(s)$; and (2) use the scalar product (5.3) to find the basis $\Psi(s)$. We can then substitute these into (5.2) to find the dynamical system of the center manifold.

In section 4, we saw that assuming a solution of the form $\mathbf{y} = \mathbf{v}e^{\lambda t}$ for the linear delayed system (4.4) yielded the eigenvector equation

$$(A + Be^{-\lambda\tau} - \lambda I)\mathbf{v} = \mathbf{0}. \tag{5.4}$$

Setting $\lambda = i\omega_c$ and $\tau = \tau_c$ and solving for the eigenvector $\mathbf{v} = (v_1, v_2, v_3, v_4)$ in the standard way, we obtain

$$\mathbf{v} = \begin{pmatrix} v_1 \\ v_2 \\ v_3 \\ v_4 \end{pmatrix} = \begin{pmatrix} -(g + \frac{4}{3}\omega_c^2 l) \\ \omega_c^2 \\ -i\omega_c(g + \frac{4}{3}\omega_c^2 l) \\ i\omega_c^3 \end{pmatrix} v_0, \tag{5.5}$$

where $v_0$ is an arbitrary constant.

Let $\phi(s) = \mathbf{v}e^{i\omega_c s}$, $-\tau_c \le s \le 0$, where $\mathbf{v}$ is given by (5.5). The matrix $\Phi(s) = [\phi(s), \bar{\phi}(s)]$ then forms a basis for the subspace $P$.

Note that for the scalar product (5.3), $\langle \bar{\psi}(s), \phi(s) \rangle = \overline{\langle \psi(s), \bar{\phi}(s) \rangle}$ and $\langle \bar{\psi}(s), \bar{\phi}(s) \rangle = \overline{\langle \psi(s), \phi(s) \rangle}$, since the entries of $B$ are real.

Let $\psi(t) = \mathbf{l}e^{-i\omega_c s}$, $0 \le s \le \tau_c$, where $\mathbf{l}$ is a constant vector. We will choose $\mathbf{l}$ so that the matrix $\Psi(s) = [\psi(s), \bar{\psi}(s)]^T$ forms a basis for the linear space of the (formal) adjoint problem. This means we must choose $v_0$ and $\mathbf{l}$ so that

$$\langle \Psi, \Phi \rangle = \begin{pmatrix} \langle \psi, \phi \rangle & \langle \psi, \bar{\phi} \rangle \\ \langle \bar{\psi}, \phi \rangle & \langle \bar{\psi}, \bar{\phi} \rangle \end{pmatrix} = \begin{pmatrix} 1 & 0 \\ 0 & 1 \end{pmatrix}.$$

Consider first the off-diagonal elements:

$$\begin{aligned}\left\langle \psi(s), \bar{\phi}(s) \right\rangle &= \psi(0)\cdot\bar{\phi}(0) + \int_{-\tau_c}^{0} \psi(s+\tau_c) B \bar{\phi}(s)\, ds \\ &= \mathbf{l}\cdot\bar{\mathbf{v}} + \int_{-\tau_c}^{0} \mathbf{l} e^{-i\omega_c(s+\tau_c)} B \bar{\mathbf{v}} e^{-i\omega_c s}\, ds \\ &= \frac{1}{2i\omega_c}\mathbf{l}(2i\omega_c I + Be^{i\omega_c\tau_c} - Be^{-i\omega_c\tau_c})\bar{\mathbf{v}} \\ &= -\frac{1}{2i\omega_c}\mathbf{l}(A + Be^{-i\omega_c\tau_c} - i\omega_c I)\bar{\mathbf{v}} + \frac{1}{2i\omega_c}\mathbf{l}\overline{(A + Be^{-i\omega_c\tau_c} - i\omega_c I)\mathbf{v}} \\ &= -\frac{1}{2i\omega_c}\mathbf{l}(A + Be^{-i\omega_c\tau_c} - i\omega_c I)\bar{\mathbf{v}} + \frac{1}{2i\omega_c}\mathbf{l}\cdot\mathbf{0}.\end{aligned}$$

Thus, if we require $\mathbf{l} = (l_1, l_2, l_3, l_4)$ to be such that

$$\mathbf{l}(A + Be^{-i\omega_c\tau_c} - i\omega_c I) = \mathbf{0}, \tag{5.6}$$

then $\langle \psi(s), \bar{\phi}(s)\rangle = 0 = \langle \bar{\psi}(s), \phi(s)\rangle$. Equation (5.6) is easily solved to yield

$$\mathbf{l} = \left(\omega^2\alpha_1, \omega^2\alpha_2 - g(\omega^2 + \alpha_1 + i\omega\alpha_3), \omega(\omega\alpha_3 - i\alpha_1), \frac{4}{3}\omega l(\omega\alpha_3 - I(\omega^2 + \alpha_1))\right) l_0, \tag{5.7}$$

where

$$\alpha_1 = \frac{4d_1 e^{-i\omega_c\tau_c}}{m+4M},\ \alpha_2 = \frac{4d_2 e^{-i\omega_c\tau_c} - 3mg}{m+4M},\ \alpha_3 = \frac{4(d_3 e^{-i\omega_c\tau_c} - \beta - \epsilon)}{m+4M},$$

and $l_0$ is an arbitrary constant.

Now consider the diagonal elements. Using the expressions (5.5) and (5.7) and simplifying with Maple [27], we find

$$\begin{aligned}\langle \psi(s), \phi(s)\rangle &= \mathbf{l}\cdot\mathbf{v} + \int_{-\tau_c}^{0} \mathbf{l} e^{-i\omega_c(s+\tau_c)} B \mathbf{v} e^{i\omega_c s}\, ds \\ &= \mathbf{l}(I + e^{-i\omega_c\tau_c}\tau_c B)\mathbf{v} \\ &= \mathbf{l}(A + Be^{-i\omega_c\tau_c} - i\omega_c I)\mathbf{v}\tau_c + \mathbf{l}\left(I\left(i\omega_c + \frac{1}{\tau_c}\right) - A\right)\mathbf{v}\tau_c \\ &= \mathbf{l}\left(I\left(i\omega_c\tau_c + 1\right) - A\tau_c\right)\mathbf{v} \\ &= l_0 v_0 \eta,\end{aligned}$$

where

$$\begin{aligned}\eta = \frac{4}{3}&\left(\frac{4(\beta+\epsilon)l\tau}{m+4M} + l\right)\omega^6 + \left(\frac{4(\beta+\epsilon)g\tau}{m+4M} + \alpha_2 - g - \frac{4}{3}l\alpha_1\right)\omega^4 - 3g\alpha_1\omega^2 \\ &+ i\left(\frac{4}{3}l\tau\omega^7 + \frac{4(M+m)g\tau}{m+4M}\omega^5 - 2g\alpha_3\omega^3\right).\end{aligned}$$

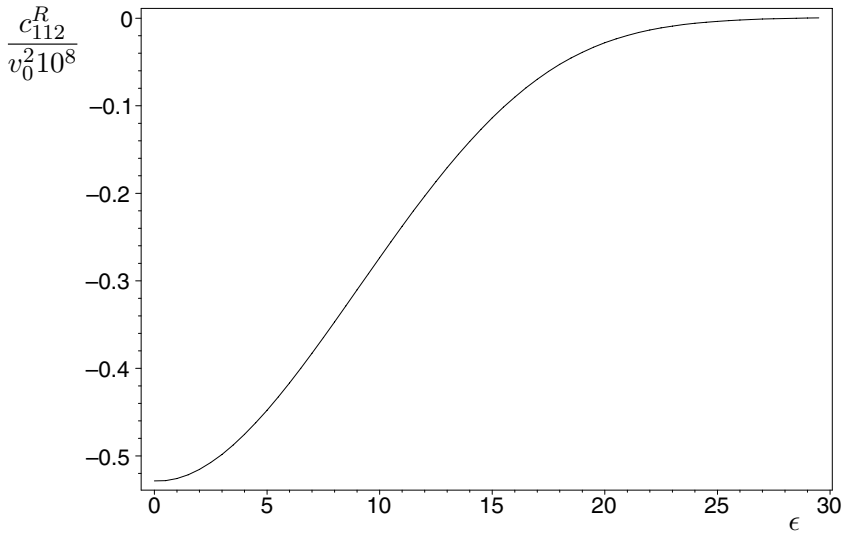


**Figure 7.** *Value of the criticality coefficient, $c^R_{112}$, as a function of the damping parameter, $\epsilon$.*

If we let $l_0 = (v_0\eta)^{-1}$, the conditions $\langle\psi(s), \phi(s)\rangle = 1 = \langle\bar{\psi}(s), \bar{\phi}(s)\rangle$ will be satisfied. This leaves one free parameter $v_0$.

To find the dynamical system of the center manifold, we need only to consider the first component of (5.2):

$$\begin{aligned}\dot{z} &= i\omega_c z + \mathbf{l}\cdot\mathbf{F}\left(\Phi(0)\mathbf{W} + \Phi(-\tau_c)\mathbf{W}\right)\\ &= i\omega_c z + c_{111}z^3 + c_{112}z^2\bar{z} + c_{122}z\bar{z}^2 + c_{222}\bar{z}^3 + O(|z|^5).\end{aligned}$$

Setting $z = x + iy$ and $c_{jkl} = c^R_{jkl} + ic^I_{jkl}$ yields the dynamical system of the center manifold in real coordinates

$$\begin{aligned}\dot{x} &= -\omega_c y + (c^R_{111} + c^R_{112} + c^R_{122} + c^R_{222})x^3 + (-3c^R_{111} + c^R_{112} + c^R_{122} - 3c^R_{222})xy^2 + O(\|\mathbf{x}\|^5),\\ \dot{y} &= \omega_c x + (3c^R_{111} + c^R_{112} - c^R_{122} - 3c^R_{222})x^2 y + (-c^R_{111} + c^R_{112} - c^R_{122} + c^R_{222})y^3 + O(\|\mathbf{x}\|^5).\end{aligned}$$

It can be shown that $c_{111} = c_{222}$ and $c_{112} = c_{122}$ and hence that the criticality of the Hopf bifurcation is determined by the quantity $c^R_{112}$ [10, p. 152]. Using Maple, we determined $\Phi$ and $\Psi$, as indicated above, for the parameter values of Table 2 and for $0 \le \epsilon \le 15$. As can be seen in Figure 7, the value of $c^R_{112}$ varies with $\epsilon$ but is always negative for the physically reasonable range. (Note that the value of $v_0$ does not affect the sign of $c^R_{112}$.) We thus conclude that the Hopf bifurcation is supercritical [10, p. 152]. This analysis is consistent with the experimental results presented in the previous section.

We performed numerical simulations on the nonlinear model (1.5) using a fourth-order Runge–Kutta solver adapted for delay differential equations, available through the package XPPAUT [7]. We used parameters as in Table 2 with $\epsilon = 10.6$ and $\tau = 0.061$ or $\tau = 0.063$, i.e., just below or just above the critical delay. For each set of parameter values we show the results of two simulations with initial functions mimicking the initial conditions of the

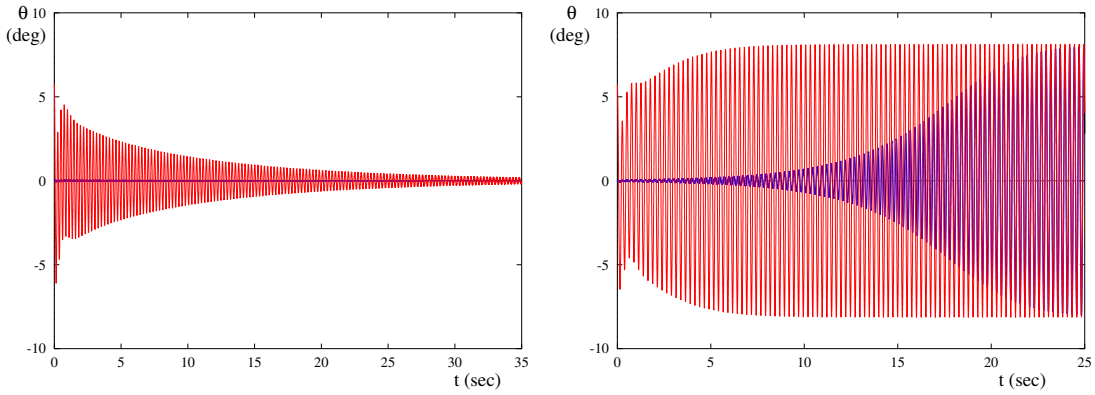


(a) $\tau = 0.061$ (b) $\tau = 0.063$

**Figure 8.** *Numerical simulations of the nonlinear model* (1.5). *Parameter values are as in Table* 2 *with* $\epsilon = 10.6$. *Initial functions are* $(x(t), \theta(t), \dot{x}(t), \dot{\theta}(t)) = (0, \theta_0, 0, 0)$, $-\tau \le t \le 0$, *with* $\theta_0 = 0.01, 0.1$ *radians.* (a) *For* $\tau = 0.061$ *the trivial solution (upright equilibrium position) is stable.* (b) *For* $\tau = 0.063$ *there is a stable periodic orbit. Shown are plots of* $\theta$ *versus* $t$*; the plots of* $x$ *versus* $t$ *are similar.*

experiment, i.e., $(x(t), \theta(t), \dot{x}(t), \dot{\theta}(t)) = (0, \theta_0, 0, 0)$, $-\tau \le t \le 0$, with $\theta_0 = 0.001$ and $\theta_0 = 0.1$ (radians). The results are shown in Figure 8. It is clear that for $\tau = 0.061$ the trivial solution (i.e., the upright equilibrium position) is stable while for $\tau = 0.063$ there is a stable periodic orbit. This supports our conclusion that the model exhibits a supercritical Hopf bifurcation at the critical delay.

The experimental system also passes from stability to instability at this value of the time delay. However, the experimental system also exhibits small periodic oscillations. Again, this is likely due to unmodeled effects. In particular, as noted above, unmodeled stiction and Coloumb friction can lead to qualitatively different behavior in the model [20, 13].

**6. Discussion.** We studied a model for a pendulum system where feedback control is used to maintain the pendulum in the upright position. We designed a controller for this system and showed that if the sampling time delay is not too large, then the controller still locally stabilizes the system. Using a center manifold reduction, we showed that when the time delay is large enough, stability is lost, a supercritical Hopf bifurcation occurs, and the system has a stable limit cycle solution. Our theoretical results are supported by experimental data.

While our model reproduces most of the behavior of the experimental system, it is not perfect. In certain situations the experimental system exhibits low amplitude, low frequency oscillations not predicted by the model. We suggest that this phenomenon is due to noise exciting modes corresponding to eigenvalues with small negative real parts. An alternative explanation is the presence of stick-slip friction between the cart and the track. A thorough investigation of these ideas would require reformulating the model, and hence we leave this to future work.

The interpretation of experimental results can be subject to debate. We are convinced

that the results shown in Figure 6 support the prediction of our model that the system exhibits a supercritical Hopf bifurcation. However, it is also possible to interpret this figure as showing bistability between a steady-state and periodic orbit. This is not something we observe in our model. Thus this latter interpretation might suggest that there are unmodeled nonlinear effects in the experimental system.

The study of delay induced bifurcations has exploded in recent years. Much of this work has focused on analyzing models for physical systems with very little on experimental systems, the exceptions being lasers (e.g., [4, 25]) and circuits (e.g., [16, 26]). We believe ours is the first paper to demonstrate a delay induced Hopf bifurcation both theoretically and experimentally in a mechanical system.

## REFERENCES


[1] F. Atay, *Balancing the inverted pendulum using position feedback*, Appl. Math. Lett., 12 (1999), pp. 51–56.

[2] J. Cabrera and J. Milton, *On-off intermittency in a human balancing task*, Phys. Rev. Lett., 89 (2002), 158702.

[3] J. Cabrera and J. Milton, *Human stick balancing: Tuning Lévy flights to improve balance control*, Chaos, 14 (2004), pp. 691–698.

[4] R. Dykstra, A. Rayner, D. Tang, and N. Heckenberg, *Controlling chaos in a single-mode laser*, in IQEC 98 Technical Digest, Summaries of Papers Presented at the International Quantum Electronics Conference, 1998, pp. 114–115.

[5] L. El'sgol'ts, *Introduction to the Theory of Differential Equations with Deviating Arguments*, Holden-Day, San Francisco, 1966.

[6] E. Eniko and G. Stépán, *Microchaotic motion of digitally controlled machines*, J. Vibration and Control, 4 (1998), pp. 427–443.

[7] B. Ermentrout, *XPPAUT*5.85 – *The Differential Equations Tool*, Department of Mathematics, University of Pittsburgh, Pittsburgh, PA, 2002, http://www.math.pitt.edu/~bard/xpp/xpp.html.

[8] T. Faria and L. Magalhães, *Normal forms for retarded functional differential equations with parameters and applications to Hopf bifurcation*, J. Differential Equations, 122 (1995), pp. 181–200.

[9] M. Golubitsky, I. Stewart, and D. Schaeffer, *Singularities and Groups in Bifurcation Theory*, Vol. 2, Springer-Verlag, New York, 1988.

[10] J. Guckenheimer and P. Holmes, *Nonlinear Oscillations, Dynamical Systems and Bifurcations of Vector Fields*, Springer-Verlag, New York, 1983.

[11] J. Hale and S. Verduyn Lunel, *Introduction to Functional Differential Equations*, Springer-Verlag, New York, 1993.

[12] G. Haller and G. Stépán, *Micro-chaos in digital control*, J. Nonlinear Sci., 6 (1996), pp. 415–448.

[13] R. Hirschorn and G. Miller, *Control of nonlinear systems with friction*, IEEE Trans. Contr. Syst. Technol., 7 (1999), pp. 588–595.

[14] L. Kollár, G. Stépán, and S. Hogan, *Sampling delay and backlash in balancing systems*, Periodica Polytechnica Ser. Mech. Eng., 44 (2000), pp. 77–84.

[15] V. Kolmanovskii and A. Myshkis, *Introduction to the Theory and Applications of Functional Differential Equations*, Math. Appl. (Soviet Ser.) 463, Kluwer, Dordrecht, The Netherlands, 1999.

[16] A. Kuboshima and T. Saito, *On a chaos generator including switched inductor with time delay*, in Proceedings of 1997 IEEE International Symposium on Circuits and Systems, Vol. 2, IEEE Circuits and Systems Society, Piscataway, NJ, 1997, pp. 9–12.

[17] K. Morris, *An Introduction to Feedback Controller Design*, Harcourt/Academic Press, New York, 2001.

[18] K. Morris and J. Juang, *Dissipative controller design for second-order dynamic systems*, in Control of Flexible Structures, K. Morris, ed., AMS, Providence, RI, 1993, pp. 71–90.

[19] I. Ncube, S. Campbell, and J. Wu, *Change in criticality of synchronous Hopf bifurcation in a multiple-delayed neural system*, in Dynamical Systems and Their Applications in Biology, Fields Inst. Commun. 36, AMS, Providence, RI, 2003, pp. 17–193.

[20] H. Olsson and K. Astrom, *Friction generated limit cycles*, IEEE Trans. Contr. Syst. Technol., 9 (2001), pp. 629–636.
[21] Quanser Consulting Inc., *IP-02 Self-Erecting, Linear Motion Inverted Pendulum*, Markham, ON, Canada, 1996.
[22] J. Sieber and B. Krauskopf, *Bifurcation analysis of an inverted pendulum with delayed feedback control near a triple-zero eigenvalue singularity*, Nonlinearity, 17 (2004), pp. 85–103.
[23] G. Stépán, *Retarded Dynamical Systems*, Pitman Res. Notes Math. Ser. 210, Longman Group, Essex, UK, 1989.
[24] G. Stépán and L. Kollár, *Balancing with reflex delay*, Math. Comput. Modelling, 31 (2000), pp. 199–205.
[25] S. Vladimir, V. Udaltsov, J.-P. Goedgebuer, L. Larger, and W. Rhodes, *Dynamics of non-linear feedback systems with short time-delays*, Optics Communications, 195 (2001), pp. 187–196.
[26] X. Wang, G.-Q. Zhong, K.-S. Tang, K. Man, and Z. Liu, *Generating chaos in Chua's circuit via time-delay feedback*, IEEE Trans. Circuits Systems I Fund. Theory Appl., 48 (2001), pp. 1151–1156.
[27] Waterloo Maple Inc., *Maple* VII, Waterloo, ON, Canada, 2001.
[28] W. Wischert, A. Wunderlin, A. Pelster, M. Olivier, and J. Groslambert, *Delay-induced instabilities in nonlinear feedback systems*, Phys. Rev. E (3), 49 (1994), pp. 203–219.